Liquid-Phase Synthesis of EuS Nanocrystals and Their Physical Properties

Supitcha Thongchant, Yasuchika Hasegawa, Yuji Wada, and Shozo Yanagida*

Department of Material and Life Science, Graduate School of Engineering, Osaka University, 2-1 Yamadaoka, Suita, Osaka 565-0871, Japan

Received: August 8, 2002; In Final Form: November 15, 2002

The first EuS nanocrystals were prepared by the reaction of europium metal and H_2S in liquid ammonia. X-ray diffraction (XRD) patterns and TEM images supported the formation of nanoscaled EuS crystals with average size of 20.4 nm. The nanocrystals showed blue shift compared with previously reported EuS films. The Curie point of EuS nanocrystals (16.6 K) was the same as that of the corresponding bulk compound, but a decreasing of magnetic moment was found because of the specific surface condition of the nanocrystals.

Introduction

There has been significant interest in the ferromagnetism of EuO and EuS from the viewpoint of the ideal Heisenberg model. *4f* Electrons distributed between the conduction band and the valence band lead to the spin moments for the Eu(II) ions.[1,2] Generally bulk EuO and EuS are prepared by solid-phase reactions of europium metal (or Eu_2O_3) and chalcogens at high temperature (>1000 °C).[3−6]

It is known that crystal size affects optomagnetic and luminescent properties of europium chalcogenides.[7−9] Especially, EuO and EuS nanocrystals have a large potential as optomagnetic and luminescent materials.[10−12] However, chemical and physical instability of their surface constitute an obstacle to the synthesis and isolation of europium chalcogenides nanocrystals. In preparation of nanoscale semiconductors, liquid-phase reactions are useful, because solvent and surfactant prevent the aggregation of particles and control crystal growth.[13−16] By liquid-phase reaction, we succeeded in preparing the first EuO nanocrystals[17] and found that the magnetic susceptibility in EuO nanocrystals increased upon irradiation with UV light.[9]

In this work, we report a novel method for preparation of high quality EuS nanocrystals using gaseous H_2S in liquid ammonia. We have identified EuS nanocrystals and obtained essential physical properties by XRD, TEM, ICP-ES, FT-IR, and UV−Vis. Furthermore, we observed that the change of their magnetic properties may depend on the morphology of the nanocrystals.

Experimental Section

Materials. Europium metal (Eu 99.9%) was obtained from Strem Chemicals. Hydrogen sulfide (pure H_2S) and ammonia (NH_3 99.9%) were purchased from Sumitomo-seika and Iwatani-neriki, respectively. The standard europium solution (1000 ppm) and sodium sulfate anhydrous (Na_2SO_4 99.0%) were purchased from Wako. All of the chemicals were reagent grade and were used as received.

Preparation of EuS Nanocrystals. Europium metal (0.3 g) was added to liquid ammonia (50 mL, −78 °C) in a reaction flask. The color of the solution turned into deep blue with the dissolution of europium. H_2S gas was introduced into the solution through bubbling until the color of the solution changed to yellow. Liquid ammonia was removed by evaporation at room temperature in 1.5 h. The resulting product was purple-black powder.

Apparatus. X-ray diffraction patterns were recorded on a Rigaku X-ray Diffractometer Multiflex using monochromate Cu Kα radiation. The measurement conditions were 40 kW/40 mA, scan speed 3°/min, sampling width 0.1°, in air, at room temperature. Transmission Electron Microscopy (TEM) images were obtained with a Hitachi H-9000 TEM equipped with a tilting device (±10 degrees) and operating at 300 kV (C_s = 0.9 nm). Images were recorded under axial illumination at approximate Scherzer focus, with a point resolution better than 0.9 nm. ICP-ES analysis was performed by Horiba Ultima 2. The EuS sample was weighed and dissolved carefully in a closed glass vessel with 15 N HNO_3 then, diluted to 1 N HNO_3 solution. The standard europium and sulfur solution were prepared from europium standard solution and heat-dried Na_2SO_4, respectively. The measurement was carried out under N_2 atmosphere. FT-IR measurements were performed at room temperature by a Perkin-Elmer system 2000 FT-IR spectrometer over the frequency range of 300−7000 cm^{-1}. The EuS sample was pressed into a pellet using KBr as a matrix. UV−Vis absorption spectra were measured on a Hitachi U-3300 spectrophotometer at room temperature. A semi-transparent EuS−KBr plate was prepared by compressing the mixture of EuS powder and KBr matrix. Magnetic measurements were carried out on superconducting quantum interference device (SQUID) magnetometer. The correlation between magnetization and temperature was recorded under magnetic field at 0.1 T, temperatures from 150 K to 10 K. The correlation between magnetization and magnetic field was recorded at 5 K under magnetic fields from −1.0 T to 1.0 T.

Results and Discussion

Characterization of EuS Nanocrystals and Reaction Mechanism. XRD measurements demonstrated well-crystallized structure of the sample (Figure 1a). Diffraction peaks 2θ = 25.9°, 30.0°, 43.0°, 50.8°, 53.4°, 62.3°, 68.7°, 70.9°, 79.0° were assigned to the (111), (200), (220), (311), (222), (400), (331), (420), (422) planes of NaCl type EuS. The intensity ratio of the diffraction patterns agreed with those of the bulk EuS. The

10.1021/jp021850z CCC: $25.00
Published on Web 02/15/2003

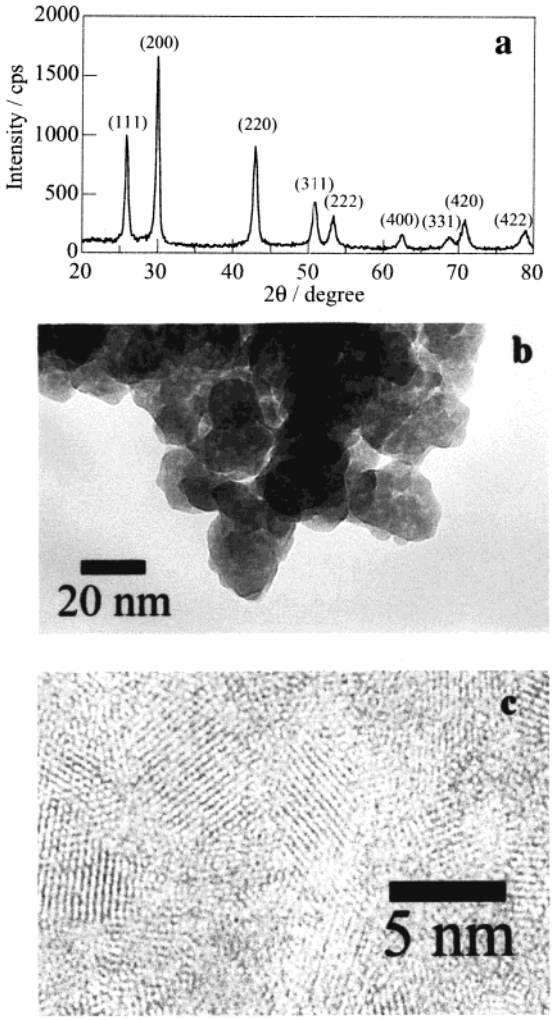

Figure 1. (a) XRD patterns, (b) the low-resolution TEM image, (c) the high-resolution TEM image of the EuS nanocrystals.

average size of EuS particles was calculated by the Scherer equation from XRD spectra (eq 1).

$$D_{hkl} = K\lambda/\beta_{1/2}\cos\theta \quad (1)$$

where D_{hkl} is the average diameter, λ is the wavelength of the X-ray, $\beta_{1/2}$ is the full width at half-maximum (fwhm) of the diffraction peak, and K is the constant. In the case of the EuS sample, we used the fwhm of $2\theta = 30.0°$, which corresponds to the Bragg diffraction from the EuS (200) planes. The average size of EuS particles was calculated to be 20.4 nm.

A TEM image of EuS is shown in Figure 1b. We observed EuS nanocrystals with average size about 20 nm, consistent with crystal size from Scherer equation. In the high-resolution image, we found a lot of tiny EuS particles (~5 nm) stacking on top of each other on the surface of the samlples (Figure 1c). The lattice fringes are indicative of the crystalline nature of the particles. A distance between the fringes was attributed to the (200) plane of EuS crystals (2.95 Å). The results indicated that liquid-phase synthesis in ammonia gave the smallest EuS nanocrystals of all the reported ones.

The reaction mechanism is shown in Scheme 1. After addition of europium metal to liquid ammonia, the color of the solution turned to deep blue because of the formation of solvated electrons ($e^{-}_{ammonia}$) and Eu(II) ions (Scheme 1, step 1**)**.[18,19] The Eu(II) ions in liquid ammonia are stable at low temperature.[20] H_2S gas diluted with argon was introduced into the solution

SCHEME 1

$$Eu(0) + NH_3 \longrightarrow Eu(II) + 2\,e^{-}_{ammonia} \quad (1)$$
$$H_2S + NH_3 \longrightarrow HS^- + NH_4^+ \quad (2)$$
$$HS^- + NH_3 \longrightarrow S^{2-} + NH_4^+ \quad (3)$$
$$NH_4^+ + e^{-}_{ammonia} \longrightarrow 2NH_3 + 1/2H_2 \quad (4)$$
$$Eu(II) + S^{2-} \longrightarrow Eu(II)S \quad (5)$$

SCHEME 2

$$Eu + S \xrightarrow[-78^oC]{NH_3,\ 12\ h} EuS + Eu_3S_4$$

through bubbling, resulting in an immediate color change into yellow. In liquid ammonia, H_2S acts as an acid that dissociated into HS^- and S^{2-} (Scheme 1, steps 2 and 3**)**. The yellow color was observed after introduction of H_2S. As long as the system was kept at −78 °C, further color change was not observed. The purple-black color of EuS from the reaction of Eu(II) and S^{2-} was observed after evaporation of liquid ammonia (Scheme 1, step 5**)**. The observed tiny EuS nanocrystals on the surface were probably generated by rapid crystal growth at the end of evaporation of liquid ammonia.

On the other hand, the synthesis of bulk EuS in liquid ammonia has been reported as shown in Scheme 2.[21] This reaction takes a long time (12 h) and is accompanied by the crystal growth of side products such as Eu_3S_4 in addition to un-reacted elements and elemental species such as europium and sulfur powder. Sulfur powder in liquid ammonia has lower reactivity than gaseous H_2S so that H_2S is the more appropriate reagent for preparation of EuS nanocrystals in liquid ammonia.

FT-IR and UV−Vis Spectra. Elemental analysis of EuS nanocrystals by ICP-ES revealed that the molar ratio of Eu(II)/S^{2-} was 1.00:1.01 (±0.01). The result implied high quality of the EuS nanocrystals. On the other hand, it was found earlier that shapes of IR spectra of europium chalcogenides depend strongly on the purity of the samples.[22−24] In the case of EuO, Shafter et al. prepared EuO samples under several conditions and classified them into 5 types (consisting of 28 minor types) based on the composition from the complexometric titration (EDTA) method.[22] They found that IR spectra and conductivity results depended and varied with the composition of EuO samples. In 1969, Verreault[23] and Bush et al.[24] reported that the impurity and defects in EuSe and EuTe increased the intensity and caused a new absorption peak of IR absorption. EuO, EuSe, and EuTe exhibited the same tendency that a stoichiometric sample is more transparent in the UV−IR region than the samples with composition defects.

From the previous reports, it could be predicted that a EuS sample with stoichiometric composition would show low IR absorption. In the FT-IR spectrum of our EuS nanocrystals, there was only a broad absorption band at 340 cm^{-1}, but no absorption band of S−H or N−H stretches (Figure 2a). The absorption band at 340 cm^{-1}, attributed to the Eu−S bond, was close to the value reported by Parkin and Fitzmaurice[21] (Figure 2b). In the EuS nanocrystals, no absorption from Eu^{3+} ions (3120 and 4820 cm^{-1}) or free carriers based on the S^{2-} deficiency (broad absorption below 3000 cm^{-1}) was observed. The FT-IR result agreed with the elemental analysis result and implied that the EuS nanocrystals have stoichiometric composition.

The absorption spectrum of the EuS nanocrystals in the UV−Vis region is shown in Figure 2c. Two absorption peaks could be observed at 665 nm, 400 nm, and below 240 nm. The EuS film (thickness: 0.520 μm) reported by Suits and Argyle[25] showed absorption peaks at 850 nm, 540 nm, and below 300 nm. On the other hand, The EuS film (thickness: 0.165 μm)

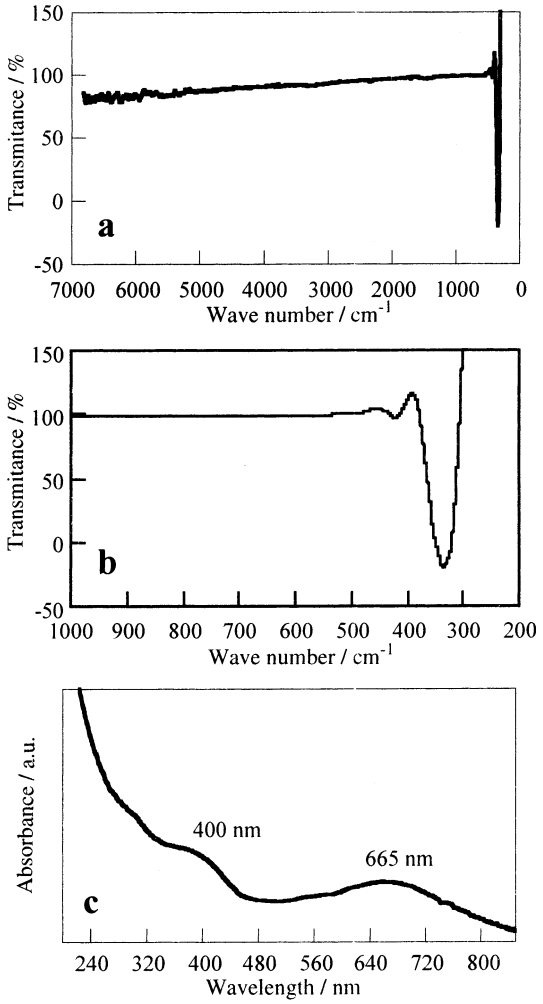

Figure 2. (a) FT-IR spectrum at whole scale, (b) FT-IR spectrum at 200−1000 cm^{-1}, (c) UV−Vis absorption spectrum, of the EuS nanocrystals.

reported by Guntherodt et al. showed absorption peaks at 540 and 267 nm.[26] The absorptions of two films were possibly consistent, although the weak 850-nm absorption was not identified in the IR spectrum of the 0.165-μm EuS film. When compared with the 0.520-μm films, the EuS nanocrystals showed blue shift by 185 nm for the 665-nm peak and 140 nm for the 400-nm peak. The blue shift in EuS nanocrystals might be partly due to the quantum size effect. However, the quantum size effect alone of the semiconductor cannot give a satisfactory explanation for the unusual large blue shift in the 20-nm EuS nanocrystal. Note that absorption of europium chalcogenides is derived from $4f^7(^8S_{7/2})-4f^6(^7F_J)5d(t_{2g})^6$ electron transition of Eu(II) ion, not from an indirect transition between valence and conduction band.[27,28] Thus the optical properties of europium chalcogenides are not always the same as those of other semiconductors. For example, absorption spectra of europium chalcogenides showed red shift at low temperatures near the Curie point.[2,27,28] The ionic $f-d$ transition is sensitive to the environment of the crystal field because the energy level of the d orbital is easily affected by the ion environment. Thus the absorption of europium chalcogenides depends not only on the particle size, but also on morphology, temperature, surface environment, and magnetic field.

Bulk EuS crystals show emission spectra in the near-IR region due to $4f^7(^8S_{7/2})-4f^6(^7F_J)5d(t_{2g})^6$ transition at low temperature.[29] Compared with the emission spectrum of the bulk compound, emission of sub-nanometer EuS crystals in zeolite X was

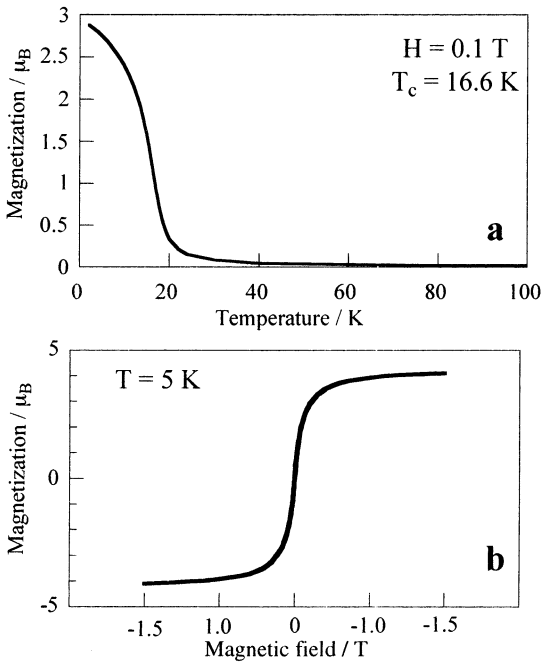

Figure 3. (a) Correlation between magnetization (M) and temperature (T) under magnetic field of 0.1 T, (b) correlation between magnetization (M) and magnetic field (H) at 5 K, of the EuS nanocrystals.

observed at room temperature and shifted to shorter wavelength.[7] However, we did not observe emission of EuS nanocrystals at room temperature. It is considered that the particle size of 20 nm would not effectively enhance the emission at room temperature.

Magnetic Measurement. By the SQUID measurement, we found that the EuS nanocrystals turned into the ferromagnetic phase at 16.6 K, consistent to the Curie point of bulk EuS (Figure 3a). However, our value for the magnetic moment per Eu(II) ion at 5 K was 4.1 m_B (Figure 3b), smaller than the expected value of 7.0 m_B for the $^8S_{7/2}$ state of Eu(II) at 0 K. In the range of 10−100 nm, ferromagnetic nanoparticles are usually composed of single domain structure.[30−32] The scale of 20 nm is probably effective in creating single domain structure in the EuS nanocrystals. However, the complicated morphology of the of EuS nanocrystals was considered to affect the magnetic moment value, because the disorderly arrangement of tiny crystals on the surface of the nanocrystals possibly decreases the exchange interaction between Eu(II) ions.

Conclusions

The high-quality nanoscaled EuS was successfully prepared by the reaction of europium metal and hydrogen sulfide in liquid ammonia at low temperature. TEM and XRD indicated that the sample obtained consisted of 20-nm EuS crystals with tiny nanocrystals stacking on the surface. The elemental analysis result and IR spectrum suggested the high purity of the EuS nanocrystals. UV−Vis absorption of the EuS nanocrystals shifted to shorter wavelength compared with those of the reported EuS films. The blue shift is mainly caused by effects of crystal environment to $f-d$ transition of Eu(II) ions and partly from size effect. The nanocrystals showed the same Curie point (16.6 K) as the bulk EuS but with a smaller magnetic moment. Disorderly arrangement of crystals on the surface might be the reason for small magnetic moment values.

Acknowledgment. This research is supported by NEDO (New Energy Industrial Technology Development Organization)

and Grant-in-Aid for Scientific Research No. 13740397. We gratefully acknowledgment Dr. Takao Sakata for TEM measurements and Assistant Professor Hidekazu Tanaka and Mr. Youhei Yamamoto for SQUID measurements.

References and Notes

(1) Enz, U.; Fast, J. F.; van Houten, S.; Smit, J. *Philips Res. Rep.* **1962**, *17*, 451.
(2) Bush, G. *J. Appl. Phys.* **1967**, *33*, 1386.
(3) Echard, J. C. *Compt. Rend.* **1957**, *244*, 3059.
(4) Shafer, M. W. *J. Appl. Phys.* **1965**, *36*, 1145.
(5) Shafer, M. *Mater. Res. Bull.* **1972**, *7*, 603.
(6) Kaldis, E. *J. Cryst. Growth* **1968**, *3*, 146.
(7) Chen, W.; Zhang, X.; Huang, Y. *Appl. Phys. Lett.* **2000**, *76*, 2328.
(8) Tanaka, K.; Fujita, K.; Soga, N.; Qui, J.; Hirao, K. *J. Appl. Phys.* **1997**, *82*, 840.
(9) Hasegawa, Y.; Thongchant, S.; Wada, Y.; Tanaka, H.; Kawai, T.; Sakata, T.; Mori, H.; Shozo, Y. *Angew. Chem., Int. Ed.* **2002**, *42*, 2073.
(10) Greiner, J. H.; Fan, G. J. *Appl. Phys. Lett.* **1966**, *9*, 27.
(11) Tanaka, K.; Tatehara, N.; Fujita, K.; Hirao, K. *J. Appl. Phys.* **2001**, *89*, 2213.
(12) Miura, N.; Kawanishi, M.; Matsumoto, H.; Nakano, R. *Jpn. J. Appl. Phys.* **1999**, *38*, L1291.
(13) Ahmadi, T. S.; Wang, Z. L.; Green, T. C.; Henglein, A.; El-Sayed, M. A. *Science* **1996**, *272*, 1924.
(14) Murray, C. B.; Norris, D. J.; Bawendi, M. G. *J. Am. Chem. Soc.* **1993**, *115*, 8706.
(15) Manna, L.; Scher, E. C.; Alivisatos, A. P. *J. Am. Chem. Soc.* **2000**, *122*, 12700.
(16) Hosogawa, H.; Fujiwara, H.; Murakoshi, K.; Wada, Y.; Yanagida, S.; Satho, M. *J. Phys. Chem.* **1996**, *100*, 6649.
(17) Thongchant, S.; Hasegawa, Y.; Wada, Y.; Yanagida, S. *Chem. Lett.* **2001**, 1274.
(18) Warf, J. C.; Korst, W. L. *J. Phys. Chem.* **1956**, *60*, 1590.
(19) Catteral, R.; Symoms, M. C. R. *J. Chem. Soc.* **1965**, 3763.
(20) Thompson, D. S.; Schaefer, D. W.; Waugh, J. S. *Inorg. Chem.* **1966**, *5*, 325.
(21) Parkin, I. P.; Fitzmaurice, J. C. *Polyhydron* **1993**, *12*, 1569.
(22) Shafer, M. W.; Torrance, J. B.; Penny, T. *J. Phys. Chem. Solids* **1972**, *33*, 2251.
(23) Verreault, R. *Solid State Commun.* **1969**, *7*, 1653.
(24) Bush, G.; Verreault, R.; Vogt, O. *Solid State Commun.* **1970**, *8*, 617.
(25) Suits, J. C.; Argyle, B. E. *Phys. Rev. Lett.* **1965**, *14*, 687.
(26) Guntherodt, G.; Schoenes, J.; Wachter, P. *J. Appl. Phys.* **1970**, *41*, 1083.
(27) Kasuya, T.; Yanase, A. *Rev. Mod. Phys.* **1968**, *40*, 684.
(28) Freiser, M. J.; Holtzberg, F.; Methfessel, S.; Pettit, G. D.; Shafer, M. W.; Suits, J. C. *Phys. Acta* **1968**, *41*, 832.
(29) Bush, G.; Streit, P.; Wachter, P. *Solid State Commun.* **1970**, *8*, 1759.
(30) Kittel, C. *Phys. Rev.* **1946**, *70*, 965.
(31) Kittel, C. *Rev. Mod. Phys.* **1949**, *21*, 541.
(32) Tomomura, A.; Matsuda, T.; Endo, J.; Arii, T.; Mihama, K. *Phys. Rev. Lett.* **1980**, *44*, 1430.